



OPEN

## GIS-based integration of marine data for assessment and management of a highly anthropized coastal area

Luciano Bosso<sup>1,2,3,12</sup>, Simona Saviano<sup>1,12</sup>, Maria Abagnale<sup>1</sup>, Daniele Bellardini<sup>1,4</sup>, Francesco Bolinesi<sup>5</sup>, Vincenzo Botte<sup>1</sup>, Angela Buondonno<sup>1</sup>, Ylenia Carotenuto<sup>1</sup>, Raffaella Casotti<sup>1</sup>, Maria Luisa Chiusano<sup>1,5</sup>, Francesco Cipolletta<sup>1</sup>, Fabio Conversano<sup>1</sup>, Francesca De Domenico<sup>6</sup>, Gabriele Del Gaizo<sup>1,7</sup>, Vincenzo Donnarumma<sup>1</sup>, Marta Furia<sup>1</sup>, Daniele Iudicone<sup>1</sup>, Florian Kokoszka<sup>8</sup>, Federica Laface<sup>6</sup>, Priscilla Licandro<sup>1,3</sup>, Olga Mangoni<sup>5</sup>, Francesca Margiotta<sup>1</sup>, Maria Grazia Mazzocchi<sup>1</sup>, Marco Miraldo<sup>1</sup>, Marina Montresor<sup>1</sup>, Marco Pansera<sup>1,9</sup>, Cristina Pedà<sup>10</sup>, Isabella Percopo<sup>1</sup>, Francesca Raffini<sup>1</sup>, Luca Russo<sup>1</sup>, Teresa Romeo<sup>6,11</sup>, Maria Saggiomo<sup>1</sup>, Diana Sarno<sup>1,3</sup>, Anna Chiara Trano<sup>1</sup>, Jessica Vannini<sup>1</sup>, Mauro Vargiu<sup>1</sup>, Gianpaolo Zampicinini<sup>1</sup>, Adriana Zingone<sup>1</sup>, Daniela Cianelli<sup>1,3</sup>✉ & Domenico D'Alelio<sup>1,3</sup>✉

Monitoring coastal marine environments by evaluating and comparing their chemical, physical, biological, and anthropogenic components is essential for ecological assessment and socio-economic development. In this study, we conducted an integrated multivariate analysis to assess the descriptors of the Marine Strategy Framework Directive at a regional scale in the Tyrrhenian Sea (Italy), with a specific focus on the densely populated coastal zone of the Campania region. Physical, chemical, and biological data were collected and analyzed in 22 sampling sites during three oceanographic surveys in the Gulf of Gaeta (GoG), Naples (GoN), and Salerno (GoS) in autumn 2020. Our results indicated that these three gulfs were distinct overall, with GoN being more divergent and heterogeneous than GoG and GoS. The marine area studied in the GoN had more favorable hydrographic and trophic conditions and food web characteristics, except for the mesozooplankton biomass, and was closer to socio-economic factors compared to the GoS and GoG. Our analysis helped us find the key ecological features that define different sub-regions and connect them to social and economic factors, including human activities. We highlighted the relevance of primary and secondary variables in terms of the comprehensive ecological assessment of a marine area and its impact on specific socio-economic activities. These findings support the need to describe and integrate multiple descriptors at the spatial scale.

**Keywords** Campania region, Ecological assessment, Geographic information system, Good environmental status descriptors, Marine spatial planning, Marine strategy framework directive, Mediterranean basin, Spatial analysis

<sup>1</sup>Stazione Zoologica Anton Dohrn, Villa Comunale, 80121 Naples, Italy. <sup>2</sup>National Research Council of Italy, Institute for Agriculture and Forestry Systems in the Mediterranean, Piazzale E. Fermi 1, 80055 Portici, Italy. <sup>3</sup>National Biodiversity Future Center, Piazza Marina 61, 90133 Palermo, Italy. <sup>4</sup>Department of Earth, Environment and Life Sciences, University of Genoa, Corso Europa 26, 16132 Genova, Italy. <sup>5</sup>Department of Biology, University of Naples Federico II, Complesso di Monte Sant'Angelo, Via Cinthia 21, 80126 Naples, Italy. <sup>6</sup>Stazione Zoologica Anton Dohrn, Sicily Marine Centre, Villa Pace, C. da Porticatello 29, 98167 Messina, Italy. <sup>7</sup>Information and Environmental Reporting Area, Agenzia Regionale Per La Protezione Ambientale del Lazio, Via Boncompagni 101, 00187 Roma, Italy. <sup>8</sup>National Research Council of Italy, Institute of Marine Sciences, Calata Porta Di Massa - Porto Di Napoli 80, 80133 Naples, Italy. <sup>9</sup>National Research Council of Italy, Institute of Polar Sciences, Via S. Raineri 86, 98122 Messina, Italy. <sup>10</sup>Stazione Zoologica Anton Dohrn, CRIMAC, C. da Torre Spaccata, 87071 Amendolara, Italy. <sup>11</sup>Institute for Environmental Protection and Research, Via Dei Mille 46, 98057 Milazzo, Italy. <sup>12</sup>Luciano Bosso, Simona Saviano equal contribution. ✉email: daniela.cianelli@szn.it; domenico.dalelio@szn.it

Coastal marine areas support marine productivity, human health, and wealth<sup>1–3</sup>. They are socio-ecological systems whose environmental status is affected by natural and anthropogenic factors, including climate change and economic activities<sup>4,5</sup>. Monitoring coastal marine environments and evaluating their chemical, physical, biological, and anthropogenic components is essential for efficient regional ecological, social, and economic development (e.g.,<sup>6</sup>).

To promote close monitoring of marine socio-ecological systems in Europe, the European Union Marine Strategy Framework Directive (MSFD, 2008/56/CE) introduced eleven complementary “descriptors” for the “Good Environmental Status”: biodiversity, non-indigenous species, fisheries and aquacultures, food webs, eutrophication, seabed integrity, hydrographical conditions, contaminants, seafood safety, marine litter, and energy introduction into marine systems. These MSFD descriptors provide the basis for multidisciplinary approaches to environmental monitoring, ecological assessment, and natural resource management to mitigate anthropic impacts and ensure marine sustainability.

The demand for higher integration among MSFD descriptors is prevalent in policy debates but poorly developed and implemented in marine coastal management. To do an ecological evaluation of the heavily anthropized Campania coast (Mediterranean Sea, Italy), this study provides a truly “holistic” perspective using numerous descriptors. With a shoreline of about 480 km, the Campania region is a socio-ecological melting pot, with fishing areas, aquaculture plants, areas under protection<sup>7</sup>, and an invaluable historical heritage attracting millions of tourists per year<sup>8</sup>. This region is heavily exposed to anthropic pressures from the Naples metropolitan area (ca. 3 million of inhabitants<sup>7</sup>), extensive agricultural, livestock, and industrial activities at the land-sea interface, illegal dumping and discharges, and two of the largest Mediterranean ports with their infrastructures and naval traffic (Naples and Salerno)<sup>9</sup>.

### **Study area and ecological assessment rationale**

The Campania region is in southwest Italy in the south Tyrrhenian Sea (Fig. 1) and includes three main gulfs (from north to south): Gaeta, Naples, and Salerno. The Gulf of Gaeta (GoG) extends for 610 km<sup>2</sup> and includes one MPA, seven AZAs, seven drains, and the Volturno River mouth (175 km; estimated mean discharge = 40 m<sup>3</sup> s<sup>-1</sup>). The Gulf of Naples (GoN) spans 138 km<sup>2</sup> and includes one MPA, eight AZAs, seven drains, seven main naval routes, and the mouth of the Sarno River (24 km), one of the most polluted European rivers<sup>9</sup>. The Gulf of Salerno (GoS) extends for 474 km<sup>2</sup> and includes one MPA, five AZAs, one drain, one naval route, and the Sele River mouth (64 km). The physical dynamics of Campania coastal waters have been investigated for decades<sup>10,11</sup>. Pelagic production is influenced by complex circulation schemes over seasonal and interannual times (e.g.,<sup>12</sup>) caused by land runoff, bathymetry, and physical forcing from the coast and offshore (e.g.,<sup>13</sup>).

Our study for the ecological assessment of the Campania coast focused on the shelf water column (0–180 m depth), a 3-D environment at the land-sea interface that is involved in multiple socio-ecological processes, such as the presence of urban drains into the sea, seafood harvesting, shipping activities, marine recreational activities and tourism, and environmental protection<sup>14</sup>. Our sampling approach focused on marine coastal sectors that were sparsely investigated by other studies and next to metropolitan regions with varying expansions. However, the explored sectors were potentially suitable for establishing mussel aquaculture plants (Fig. 1). Our sampling activities (Tables S1–S5) occurred in late summer/early autumn (September–October 2020), a period relevant for mussel aquaculture in Campania, at the edge of the settling of juveniles in production plants and the start of the harvesting season for commercially exploited adults. We assessed the ecological state of the investigated marine sectors in the period of interest by exploring and integrating the following descriptors (see methodological details in the Materials and Methods section).

### **Hydrographical conditions**

In coastal seas such as those investigated herein, hydrographic conditions mainly depend on the seasonal circulation pattern of water masses<sup>15</sup>. We characterised these patterns in the study area by simulating the most likely surface current fields for the monitoring period with data-driven hindcast modeling<sup>16</sup>. To supplement the transport patterns, we examined the physicochemical conditions of the water column across the research area. These characteristics included temperature, salinity, and dissolved oxygen, the latter of which served as a proxy for photosynthetic activity.

### **Trophic conditions**

Eutrophication—i.e., the massive proliferation of the microscopic primary producers suspended in the water column—relies on hydrographical conditions (e.g.,<sup>17</sup>). We investigated trophic conditions in the study area by analyzing the levels of chlorophyll *a*, i.e., a proxy for photosynthetic biomass in the water column, plus the abundance of heterotrophic bacteria, which thrive in eutrophic conditions. To identify potential eutrophic and oligotrophic marine sectors, we analysed inorganic and organic nutrients, i.e., the main chemical driving factors of primary production in the water column, such as nitrogen and phosphorus compounds and silicates, essential for diatoms growth (e.g.,<sup>18</sup>).

### **Plankton biodiversity**

Hydrographical and trophic conditions are strongly linked to biodiversity<sup>19</sup>. We sampled the water column of the target areas, identified and counted under the light microscope the following three planktonic groups: i) phytoplankton, i.e., mainly photosynthetic unicellular organisms between 2 and 200 µm in size, some of which induce eutrophication and impact human health and wealth negatively through the so-called Harmful Algal Blooms (HABs), at times contaminating aquacultures and wild seafood<sup>20</sup>; ii) protozooplankton, mainly heterotrophic unicellular organisms with the same size as phytoplankton, also including mixotrophs, i.e., organisms capable of doing both predation and photosynthesis<sup>21</sup>; and iii) mesozooplankton (i.e., metazoan

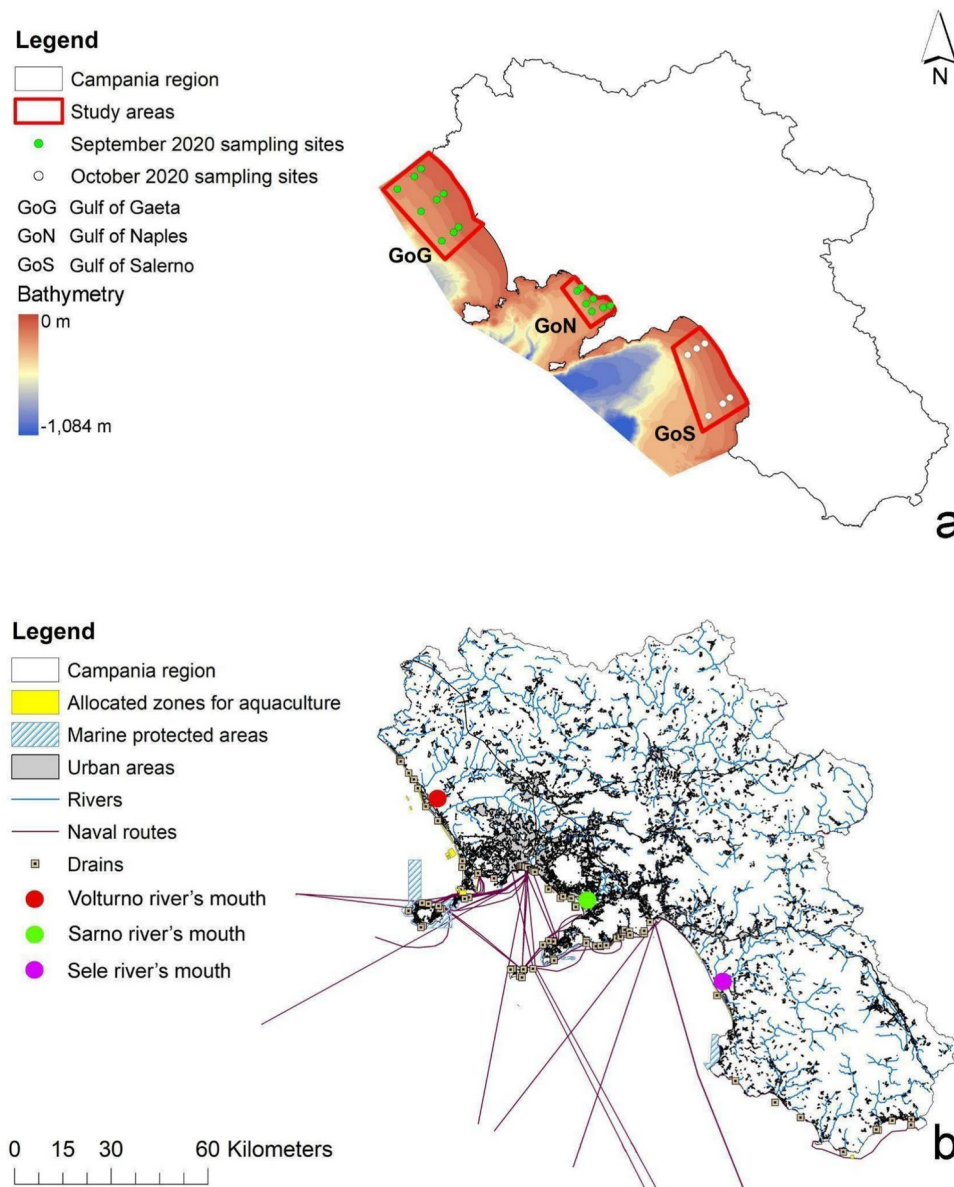


**Fig. 1.** Study areas (red lines) and sampling sites (green and white points) in the two sampling months of 2020 (a) and a map of the Campania Region with urban areas, the three rivers' mouths, Marine Protected Areas (MPAs), Allocated Zones for Aquaculture (AZAs), drains, and main naval routes (b). These maps are high-resolution; please zoom in to view more details. To optimise the display of AZAs, MPAs, and drains, we have included more thorough maps for these layers in the supplementary materials (Figure S1). These maps were generated in ArcGIS v. 10.8 (<https://www.esri.com/en-us/home>).

consumers between 200–20,000  $\mu\text{m}$  size, mainly drifted by ocean currents). We also collected marine sediments from selected sites and analysed DNA therein in search of traces of resting stages of potentially toxic phytoplankton species, whose germination can produce HABs<sup>22</sup>.

### Plankton food webs

Plankton sit at the level of basal and intermediate marine food webs, which respond more rapidly to changes in hydrographic conditions and eutrophication and establish a link between the chemical sphere of water and higher organisms commercially exploitable (e.g.,<sup>23</sup>). By summing up all taxon-specific data from our biodiversity surveys (see the previous paragraph), we explored the planktonic food web in the study areas in a simplified way by comparing the biomass of the main planktonic trophic guilds<sup>24</sup>, i.e., phytoplankton feeding both proto- and mesozooplankton and mesozooplankton preying both phyto- and protozooplankton. The ratio of their biomass can be informative of the food web state, such as the ability of the whole planktonic assemblage to provide food to macroscopic animals.

## Microscopic marine litter

In parallel with physical, chemical, and biological descriptors, we monitored microplastics, a significant form of microscopic marine litter < 5 mm in size. Micro (and nano) plastics enter the food chain via predation or filter-feeding, impacting also aquaculture<sup>25,26</sup>. In addition, microplastics represent a substrate on which different microbes can accumulate (e.g.,<sup>27</sup>), including potentially harmful ones. For these reasons, we quantified microplastic concentrations by microscopy and characterised the microbiota developing on selected pieces using Illumina sequencing and compared them with the surrounding free-living microbiota.

## Main objectives

Our main goal is to investigate, map and integrate the MSFD described in the previous paragraphs with socio-economic attributes, such as aquaculture distribution and potential contaminant sources in the study areas. To achieve this aim, we performed statistical analyses under the Geographic Information System (GIS) framework, considering sampled and measured variables plus the distance of sample points from urban areas, MPAs, AZA, rivers, drains, and naval routes. By incorporating a large amount of data (field survey, model output, remotely sensed imagery, etc.), GIS provides an effective tool for decision-makers (e.g.,<sup>28,29</sup>) that can help to model and display complex trade-offs between management alternatives, dealing with uncertainty (e.g., random processes or data deficiencies) at different spatial scales (e.g.,<sup>30</sup>). This GIS-guided integration of multiple MSFD descriptors allowed us to analyze the environmental status of Campania coastal areas. We characterised the Campania coast based on physical, chemical, biological, and socio-economic variables corresponding to nine MSFD descriptors. Over the course of two months, we arranged and conducted sampling sessions to promote data interoperability along multiple coast-to-offshore transects, across urbanised areas, river mouths, urban discharges, nearby Marine Protected Areas (MPAs), Allocated Zones for Aquaculture (AZA), and naval routes. To investigate the complementarity of MSFD descriptors in the study area and to clarify the socio-ecological context, we integrated all the numerical data from these field observations using GIS tools. We discussed the effectiveness of holistic environmental monitoring in informing policymakers at the regional level.

## Results

### Hydrographical and trophic conditions

The surface dynamic context along the Campania coast during our study (September and October 2020) is shown in Figs. 2a – 2 d. Surface current fields showed that water masses flowing from adjacent coastal areas influenced the offshore sector of the south-central Tyrrhenian Sea. The inner part showed dynamics specific to the coastal system under study. The primary local physical driver was wind stress, which also established a surface circulation that was highly reliant on wind regimes operating across the study area. Wind stress resulted in the main local physical driver and determined a surface circulation strongly dependent on wind regimes acting over the study area. In September, offshore GoG and the northern part of GoN (the Procida channel) showed high-intensity southward currents, and GoS showed a cyclonic circulation with high velocity along the coast (Fig. 2e). In October, a high-intensity northward current was present offshore GoS, entering in the south of GoN through the Bocca Piccola channel, whereas, in the GoG, we observed a southward current (Fig. 2f).

These water transport conditions were at the base of the physical and chemical differences within and among the three gulfs that we observed during our oceanographic sampling. Temperature showed typical values for the end of summer/early autumn period, and it was relatively lower near river mouths both in GoG and GoN (Fig. 3a), where salinity values were locally minimal due to freshwater inputs (Fig. 3b).

Fluorescence was highest at Naples' harbors (GoN) and GoG and GoS river mouths (Fig. 3c). Dissolved oxygen was higher in GoN and showed lower local values near the Sarno and Volturno river mouths (Fig. 3d). These patterns flanked the chemical variables involved in eutrophication processes (see below).

In the surface layer interested in eutrophication (0–10 m), inorganic nutrients like total dissolved nitrogen and dissolved inorganic nitrogen showed higher mean concentrations in the GoN, especially at coastal stations (Figs. 4a and b). The total chlorophyll *a* concentration showed coast-to-offshore gradients in the three gulfs except for the area close to the Sarno River in the GoN (Fig. 5a), with the highest values in GoN, such as also for the dissolved inorganic nitrogen, along with heterotrophic prokaryotes, possibly due to Sarno River inputs. In the other areas, bacteria peaked offshore (GoG) and at the Sele River mouth (GoS). Particulate organic carbon, including both phyto- and bacterioplankton, had the same coast-to-offshore distribution of nutrients (Fig. 4c). On average, phosphorus showed comparable concentrations in the three gulfs; silicates were higher in GoN (Fig. 4d). The silicate and microplastic values were higher close to the Sarno River mouth than in the other part of the Campania coast (Figs. 4e and 4f).

### Microplastics and the “plastisphere”

Overall, a total of ~ 9000 floating Microplastic Items (MPs) were collected from the three sampled sites. The highest concentrations (23 items m<sup>-3</sup>) were observed at the Naples site, while lower values were observed in GoG and GoS (Fig. 4f). The chemical composition of the microplastics isolated for DNA extraction was confirmed by Fourier-Transform Infrared Spectroscopy (FT-IR). Microplastics identified were polyethylene, polypropylene, and polystyrene (see Table S2). Prokaryotes thriving on microplastics shared only 55% of taxa with the free-living counterparts, suggesting that these represent a selective substrate for free-living prokaryotes. In general, both free water and microplastics were dominated by Proteobacteria and Bacteroidetes, with Rhodobacteraceae and Flavobacteriaceae as the most represented families (Figure S2). On microplastics, 38% of prokaryotic taxa were common to all sampled sites and were represented by families Vibrionaceae and Pseudoalteromonadaceae, which can potentially include harmful species. While the latter, together with Alteromonadaceae, were abundant on the microplastics from the Gulf of Naples, other families were significantly contributing to the communities in the GoS (Rhodocyclaceae and Comamonadaceae, considered markers of freshwater influence) or in the

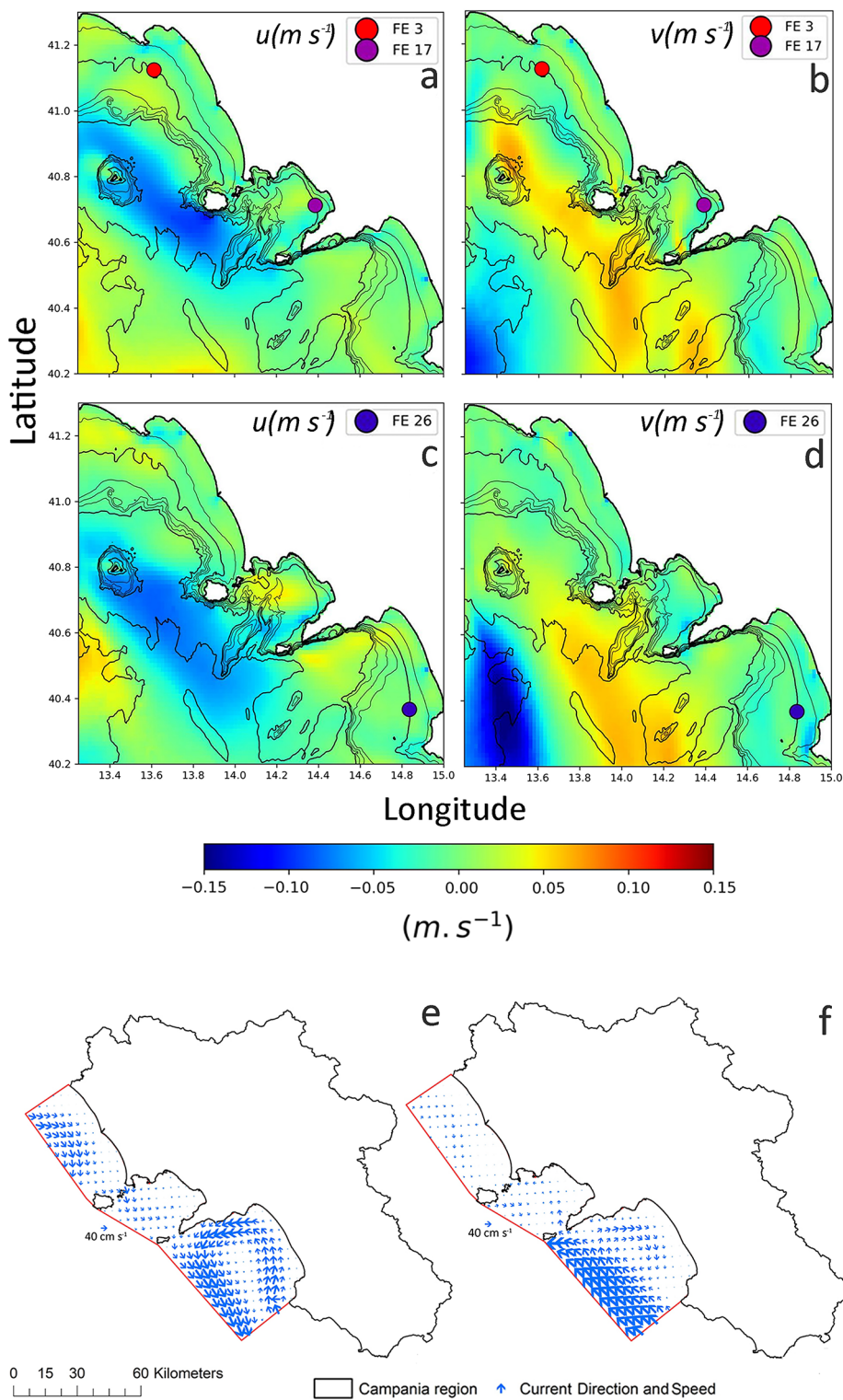


**Fig. 2.** Mean value of  $u$  ( $v$ ) velocity field component in September 2009 evaluated in the sampling stations FE3 and FE17 (Gulf of Gaeta and Gulf of Naples, respectively). Gulf of Naples Advanced Model (GNAM) data (a—b). The mean value of the  $u$  ( $v$ ) velocity field component in October 2009 was evaluated in the sampling stations FE26 (Gulf of Salerno) GNAM model data (c—d). Surface current field along the Campania coast during the sampling dates in September (e) and October (f) 2020, Copernicus Marine Environment Monitoring Service data. These maps were generated in ArcGIS v. 10.8 (<https://www.esri.com/en-us/home>).

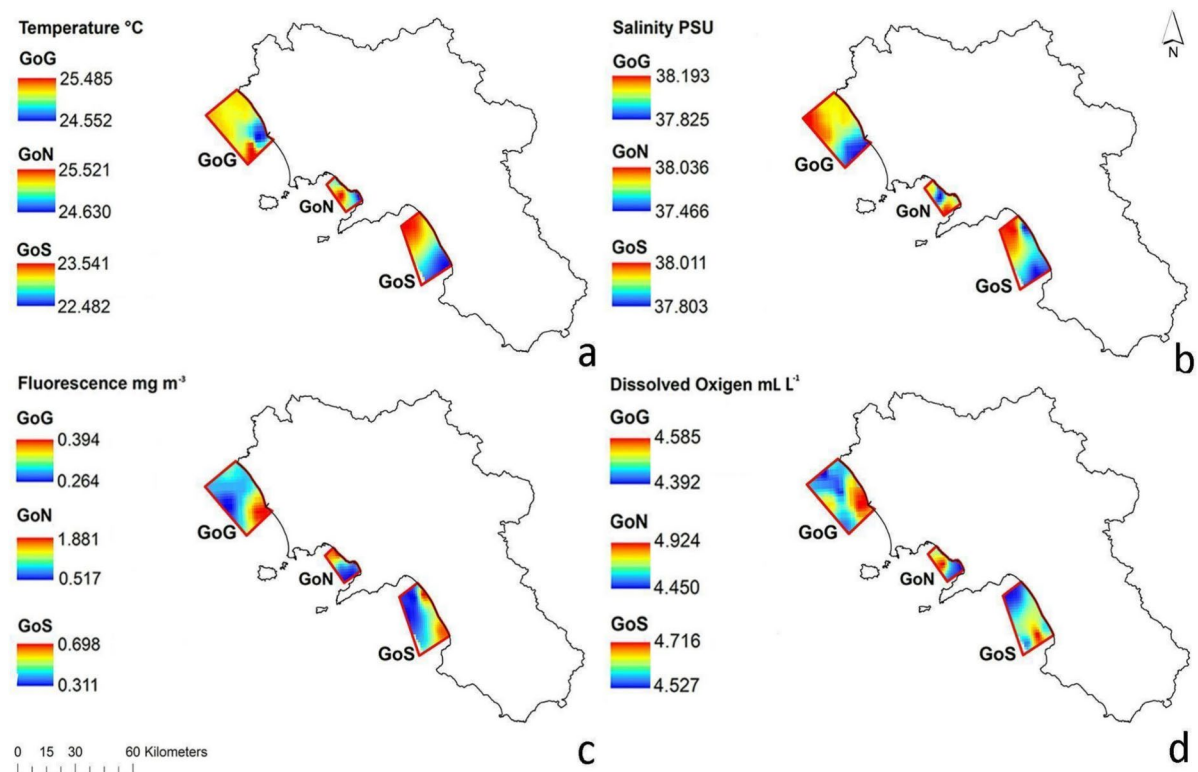


**Fig. 3.** Spatial distribution of physical variables for the Gulf of Gaeta (GoG), Gulf of Naples (GoN), and Gulf of Salerno (GoS) in the Campania Region. The panels are as follows: temperature (**a**), salinity (**b**), fluorescence (**c**), and dissolved oxygen (**d**). Note that numerical scales are different in each map. These maps are high-resolution; please zoom in to view more details. These maps were generated in ArcGIS v. 10.8 (<https://www.esri.com/en-us/home>).

GoG (Xanthomonadaceae and Paenibacillaceae, considered hydrocarbonoclastic and plastic degraders). Microeukaryotes thriving on microplastic shared 52% of the taxa with the free-living ones, while only 37% were shared between microplastic from the three sites. Taken together, most eukaryotes belonged to unknown phyla, followed by Bacillariophyta, Apicomplexa, and Chlorophyta. Among the unknown families, the main represented ones belonged to Fragilariophyceae, Apicomplexa, and Dinophyceae in the GoN; Apicomplexa, Stemonitidae, and Sphaerozooidae in the GoS; and Coscinodiscophyceae, Oomycetes, and Dinophyceae in the GoG (Table S3).

### Planktonic biodiversity

Flagellates dominated phytoplankton samples taken from the Campania water column (59–72% of the total biomass), followed by diatoms in GoN and GoG (31% and 18%, respectively) and dinoflagellates in GoS (19%). *Pseudo-nitzschia*, a bloom-forming and potentially harmful diatom genus, occurred mainly in the GoN (1.6% of total phytoplankton biomass) (Figs. 5b – 5f). Seven dinoflagellate species (*Alexandrium cf. minutum*, *Dinophysis caudata*, *Dinophysis sacculus*, *Gonyaulax spinifera*, *Karenia brevis*, *Phalacroma rotundatum*, and *Prorocentrum lima*), reported as potentially toxic, occurred at very low abundances in the study area. About protozooplankton from the Campania water column, biomass ranges were dissimilar in the three gulfs (Figs. 5b – 5f). Heterotrophic dinoflagellates dominated in the GoG and GoN (53% and 58% of the total protozooplankton biomass, respectively), and they were followed in rank by ciliates (39% and 36%, respectively) and tintinnids (2.8 and 2.6%, respectively). In GoS, ciliates were the main contributors (43%), followed by dinoflagellates (34%) and tintinnids (17%). As for mesozooplankton, higher biomass was recorded in GoG and GoN (Figs. 5b – 5f). We identified 145 taxa, with Pteropoda, Copepoda (mainly *Temora stylifera* and *Clausocalanus* juveniles), Diplostraca (*Penilia avirostris*), Chaetognatha, and Cnidaria being the main contributors to total mesozooplankton biomass. Pteropods dominated in GoG (avg. 36%), copepods (avg. 36–42%) and chaetognaths (avg. 14–18%) in GoN and GoS. The typical summer group of diplostracans was conspicuous in GoG (avg. 21%) and GoN (avg. 25%). Gelatinous cnidarians were relevant at coastal GoN (35%) and GoG (34%). The plankton taxa retrieved here were in line with the gulfs' taxonomic diversity of the last decades.

In the sediments, dinoflagellates were mostly abundant in samples collected close to the Volturno and Sarno River mouths (~ 60% and ~ 40% of taxa detected, respectively), followed by diatoms, including mainly species from the bloom-forming and resting spore-producing genus *Chaetoceros*. Dinoflagellates presented a broader diversity, with most taxa capable of producing resting stages. Overall, in the sediments, only dinoflagellates included potential HAB species, which accounted for about 10% of this group (Table S4).

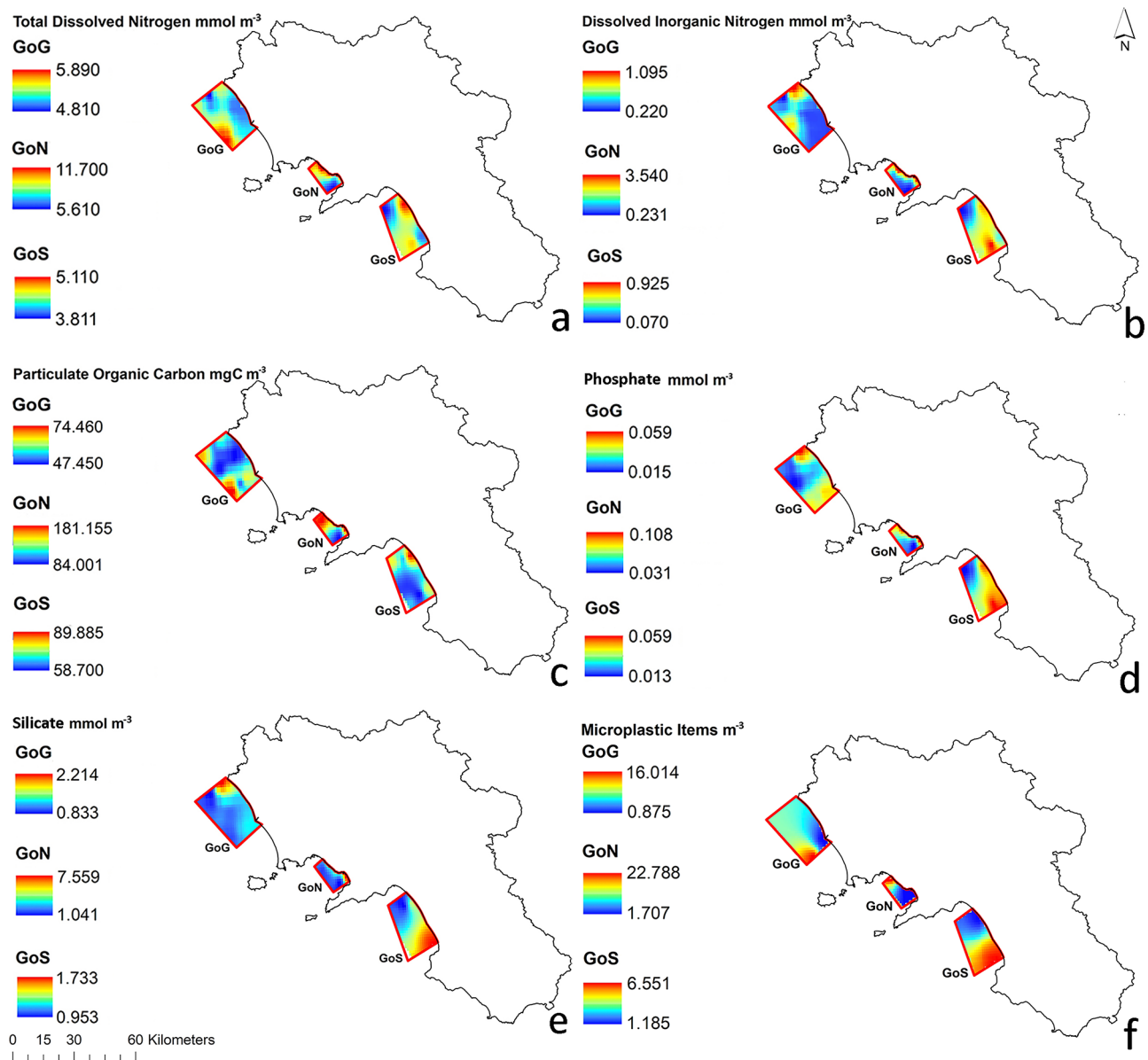


**Fig. 4.** Spatial distribution of chemical variables in the Gulf of Gaeta (GoG), Gulf of Naples (GoN), and Gulf of Salerno (GoS) in the Campania Region. The panels are as follows: total dissolved nitrogen (a), dissolved inorganic nitrogen (b), particulate organic carbon (c), phosphate (d), silicate (e), and microplastic items (f). Note that numerical scales are different in each map. These maps are high-resolution; please zoom in to view more details. These maps were generated in ArcGIS v. 10.8 (<https://www.esri.com/en-us/home>).

### Planktonic food webs

Phytoplankton and protozooplankton biomasses (Figs. 5b – 5f) reached their highest values in the GoN, with a southward decrease towards the Sarno River mouth; in the same gulf, mesozooplankton biomass was highly variable, but it reached its highest value at the coastal side of the northern sector, indicating that the distribution of planktonic animals depended on food-resources.

Analogously, in the GoS, i.e., the less productive gulf, the biomass of all trophic guilds decreased offshore. A different pattern occurred in GoG, where phytoplankton showed a positive coast-to-offshore gradient, and proto- and mesozooplankton peaked in the area interested by the Volturno River mouth, indicating top-down control. Overall, the ratio between primary producers, i.e., the phytoplankton, and their consumers, i.e., the proto- and mesozooplankton, appeared well balanced, as typically happens at the end of the summer/autumn season in temperate regions.

### Integration of descriptors and socio-ecological assessment

ANOVA analyses indicated that almost all the analysed variables were significantly different among the three gulfs (Table 1 and figures in the supplementary materials such as S4, S5, S6, and S7).

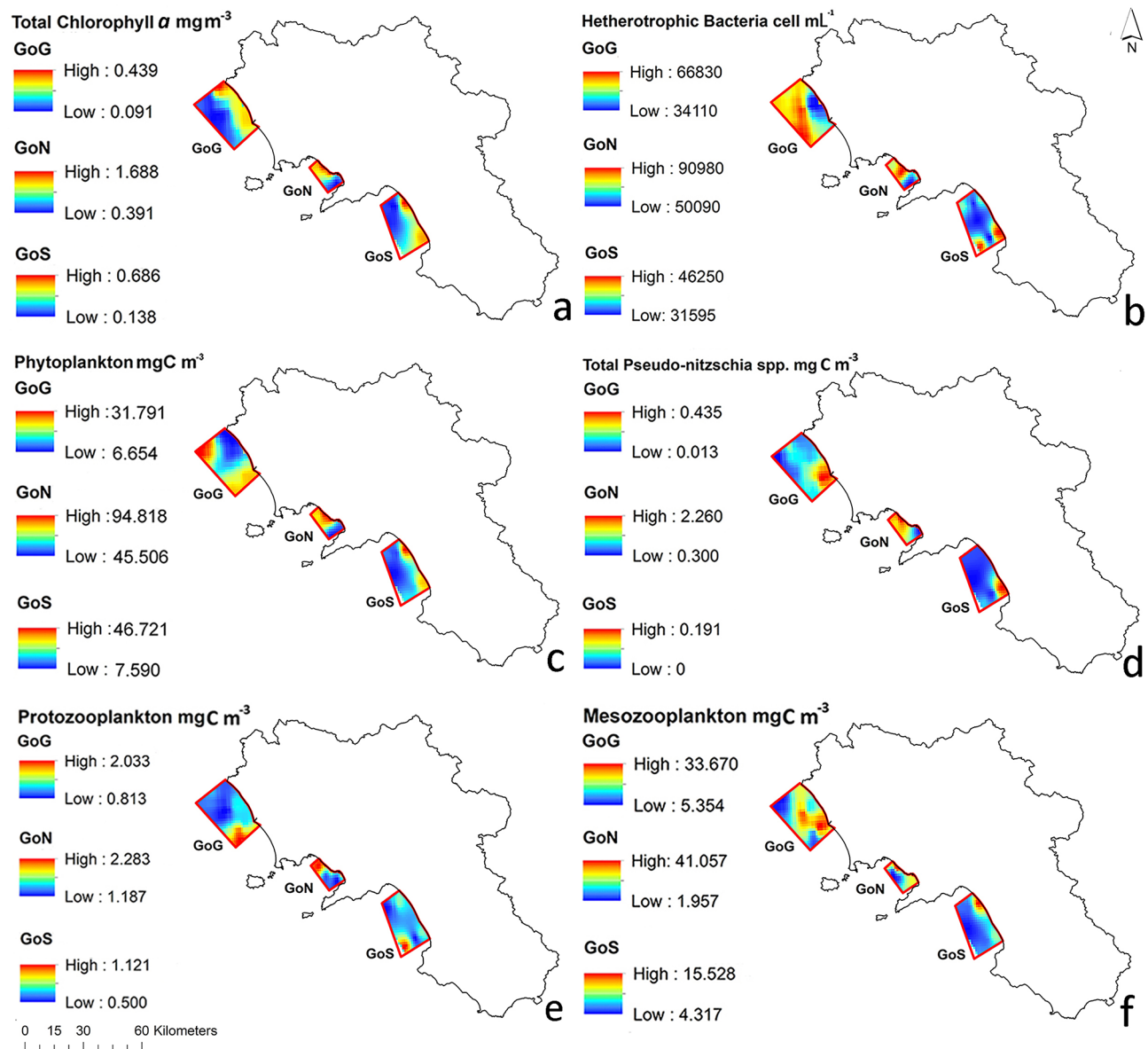


**Fig. 5.** Spatial distribution of biological variables in the Gulf of Gaeta (GoG), Gulf of Naples (GoN), and Gulf of Salerno (GoS) in the Campania Region. The panels are as follows: total chlorophyll  $\alpha$  (a), heterotrophic bacteria concentrations (b), phytoplankton carbon biomass (c), *Pseudo-nitzschia* carbon biomass (d), protozooplankton carbon biomass (e), and mesozooplankton carbon biomass (f). Note that numerical scales are different in each map. These maps are high-resolution; please zoom in to view more details. These maps were generated in ArcGIS v. 10.8 (<https://www.esri.com/en-us/home>).

The marine sector investigated in the GoN showed higher values for the hydrographic and trophic conditions and food web descriptors, except for the mesozooplankton biomass. The same area in the GoN also showed lower distances from socio-economic attributes, indicating that the GoN was the most anthropized, followed by the GoS and GoG.

The integration of different descriptors assessed that the three gulfs were environmentally divergent. Principal Component Analysis (PCA) (Fig. 6a), performed with all the variables in Table 1, showed three minimally overlapping clusters corresponding to the three gulfs whose diversity is jointly driven by multiple variables. In Dim1, explaining 41.2% of the observed variance and mostly influenced by total chlorophyll  $\alpha$ , GoN appeared as the most distinct gulf, with a limited overlap with GoG, while the other two gulfs were more like each other despite them being geographically more distant (Figure S8). GoG and GoS were more distinct in Dim2, which explained 19.3% of the observed variance and was mostly influenced by the total dissolved nitrogen (Figures S8). GoN emerged as a more heterogeneous basin compared to GoG and GoS.

When considering the physical variables alone (Fig. 6b), salinity and dissolved oxygen were negatively correlated and influenced divergence along Dim1 (54.9% of the observed variance), while temperature was

Variable	GoG		GoN		GoS	
	Mean	SD	Mean	SD	Mean	SD
Current direction (degree)	100.610 <sup>a</sup>	23.402	125.832 <sup>b</sup>	9.764	130.296 <sup>b</sup>	31.891
Current speed (m s <sup>-1</sup> )	16.559 <sup>a</sup>	4.023	5.897 <sup>b</sup>	1.104	15.396 <sup>a</sup>	13.081
Dissolved inorganic nitrogen (mmol m <sup>-3</sup> )	0.423 <sup>a</sup>	0.233	0.847 <sup>b</sup>	0.621	0.494 <sup>c</sup>	0.207
Dissolved oxygen (mL L <sup>-1</sup> )	4.483 <sup>a</sup>	0.060	4.658 <sup>b</sup>	0.138	4.595 <sup>c</sup>	0.043
Dist. from AZA (m)	7,999.265 <sup>a</sup>	5,328.913	3,452.330 <sup>b</sup>	1,834.269	7,059.620 <sup>c</sup>	4,268.518
Dist. from drains (m)	10,777.898 <sup>a</sup>	5,590.713	3,309.563 <sup>b</sup>	1,755.083	10,147.361 <sup>a</sup>	3,761.149
Dist. from MPA (m)	11,117.766 <sup>a</sup>	5,062.687	6,994.446 <sup>b</sup>	3,550.856	7,318.323 <sup>b</sup>	3,672.259
Dist. from naval route (m)	35,048.267 <sup>a</sup>	8,565.035	2,026.974 <sup>b</sup>	1,525.436	5,114.161 <sup>c</sup>	3,766.349
Dist. from river (m)	10,232.013 <sup>a</sup>	5,491.651	4,358.666 <sup>b</sup>	1,717.980	7,654.368 <sup>c</sup>	4,091.884
Dist. from urban (m)	10,101.786 <sup>a</sup>	5,657.211	3,246.920 <sup>b</sup>	1,831.726	7,423.464 <sup>c</sup>	4,097.825
Fluorescence (mg m <sup>-3</sup> )	0.318 <sup>a</sup>	0.035	0.907 <sup>b</sup>	0.399	0.449 <sup>c</sup>	0.121
Heterotrophic bacteria (cell mL <sup>-1</sup> )	53,281.520 <sup>a</sup>	9,948.987	68,425.799 <sup>b</sup>	13,536.293	36,506.763 <sup>c</sup>	4,078.818
Mesozooplankton (mgC m <sup>-3</sup> )	18.627 <sup>a</sup>	7.503	9.826 <sup>b</sup>	5.814	5.457 <sup>c</sup>	2.952
Microplastic (Items m <sup>-3</sup> )	4.763 <sup>a</sup>	3.683	5.804 <sup>a</sup>	6.793	3.904 <sup>b</sup>	1.897
Particulate organic carbon (mgC m <sup>-3</sup> )	56.560 <sup>a</sup>	6.467	128.075 <sup>b</sup>	38.058	68.177 <sup>c</sup>	7.248
Phosphate (mmol m <sup>-3</sup> )	0.032 <sup>a</sup>	0.011	0.053 <sup>b</sup>	0.017	0.038 <sup>c</sup>	0.013
Phytoplankton (mgC m <sup>-3</sup> )	17.851 <sup>a</sup>	7.600	69.814 <sup>b</sup>	18.105	16.411 <sup>a</sup>	11.016
Protozooplankton (mgC m <sup>-3</sup> )	1.204 <sup>a</sup>	0.349	1.639 <sup>b</sup>	0.376	0.700 <sup>c</sup>	0.114
<i>Pseudo-nitzschia</i> (mgC m <sup>-3</sup> )	0.164 <sup>a</sup>	0.107	1.188 <sup>b</sup>	0.412	0.033 <sup>c</sup>	0.060
Salinity (PSU)	38.029 <sup>a</sup>	0.099	37.771 <sup>b</sup>	0.140	37.901 <sup>c</sup>	0.063
Silicate (mmol m <sup>-3</sup> )	1.117 <sup>a</sup>	0.319	1.765 <sup>b</sup>	1.236	1.341 <sup>c</sup>	0.243
Temperature (°C)	25.079 <sup>a</sup>	0.210	25.104 <sup>a</sup>	0.204	23.006 <sup>b</sup>	0.358
Total chlorophyll <i>a</i> (mg m <sup>-3</sup> )	0.214 <sup>a</sup>	0.105	0.913 <sup>b</sup>	0.371	0.323 <sup>c</sup>	0.158
Total dissolved nitrogen (mmol m <sup>-3</sup> )	5.294 <sup>a</sup>	0.237	7.420 <sup>b</sup>	1.471	4.389 <sup>c</sup>	0.311

**Table 1.** Difference among the physical, chemical, biological, and anthropogenic variables used in the Principal Component Analysis and spatial analysis for/among the Gulf of Gaeta (GoG), the Gulf of Naples (GoN), and the Gulf of Salerno (GoS) in the Campania Region. The full results are available in Supplementary Materials (Figures S4, S5, S6, and S7). AZA = Allocated Zones for Aquaculture; Dist. = Distance; MPA = Marine Protected Area. Different letters in the columns (a, b and c) refer to significant differences ( $P < 0.0001$ ) among GoG, GoN and GoS.

linked to Dim2 (22.7% of the observed variance, Figure S9). Here, GoN was clearly distinct from the other two gulfs, which showed minimal overlap. GoS largely converged with GoG and GoN along Dim1, while in Dim2 it showed a more substantial separation from the other two gulfs. All three gulfs exhibited similar levels of diversity within the basins.

Among the chemical variables (Fig. 6c), total chlorophyll *a* and silicate were the most influential ones to Dim1 and Dim2, respectively, that explained 59.8 and 16.4% of the observed variance, respectively (Figure S10). GoS showed an extensive overlap with GoG and part of GoN. GoN emerged as a more distinct and strongly heterogeneous basin compared to the other two gulfs.

The three basins exhibited a clear separation in their biological variables (Fig. 6d), with GoS producing a distinct cluster and a minimal overlap between GoN and GoG. Their divergence was mostly driven by phytoplankton (Dim1, 63.5% of the observed variance) and mesozooplankton (Dim2, 21.7% of the observed variance, Figure S11). GoS appeared as a more homogeneous basin compared to GoN and GoG, which showed a large internal diversity.

Two distinct groups, corresponding to GoG and GoS plus GoN, emerged regarding variables linked to distances (not shown in the PCA figure for brevity). They were mostly related to distance from urban centers (Dim1, 72.7%) and naval routes (Dim2, 16.2%). In contrast to previous trends, GoG showed the highest internal heterogeneity, while GoN was the most homogeneous gulf (Figure S12).

A synthetic view of the multiple interrelations among the variables observed at the regional scale is visualised as a network, including both positive and negative relationships (Fig. 7). Therein, the most interrelated variables are total chlorophyll *a* and phosphate, followed by particulate organic carbon and fluorescence. Total chlorophyll *a* and phosphate appear to positively influence particulate organic carbon, fluorescence, and phytoplankton, but they are negatively affected by the whole group of distance variables that, on the other hand, are highly correlated to each other. Moreover, Temp was positively linked to protozooplankton, mesozooplankton, and heterotrophic bacteria.

## Discussion

Human activities and the overexploitation of ecosystems in coastal marine areas impact physical, chemical, and biological attributes at the local scale<sup>4</sup>. Despite the progressive improvement of knowledge about their complexity, environmental monitoring programs of coastal marine ecosystems typically consider each physical,

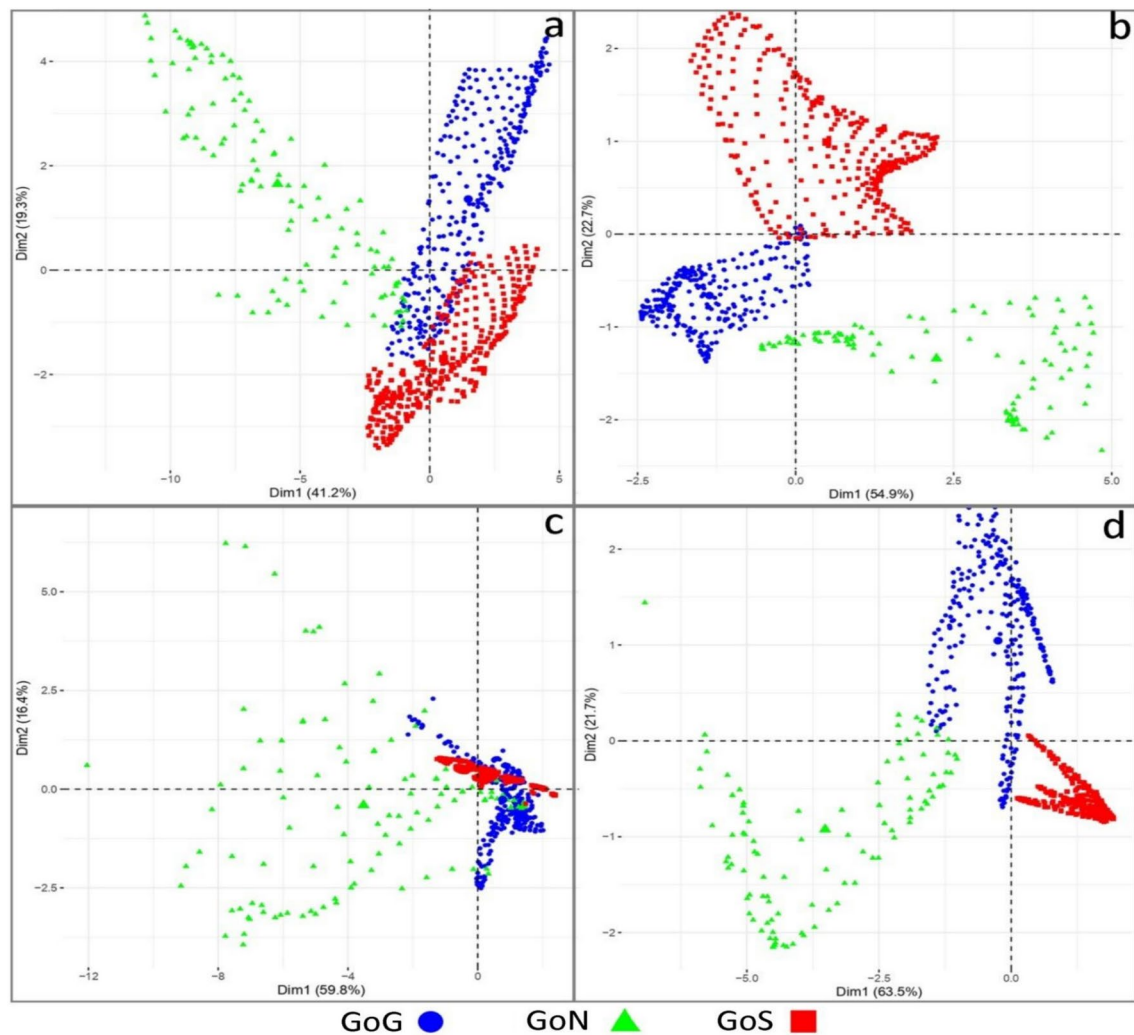


**Fig. 6.** The Principal Component Analysis (PCA) of data retrieved in the Gulf of Gaeta (GoG, blue points), the Gulf of Naples (GoN, green triangles), and the Gulf of Salerno (GoS, red squares) is shown in Fig. 1. a = PCA all variables together, including distances from the Allocated Zones for Aquaculture, drains, Marine Protected Areas, naval routes, and river mouths; b = PCA physical variables; c = PCA chemical variables; d = biological variables.

chemical, and biological dimension in isolation. Here, we show that a multidimensional analysis is more effective than an analysis using a single variable or a few *a priori* selected and conceptually poorly connected ones to assess the ecological status of a marine coastal area that is heavily, but differentially, affected by anthropogenic impact.

Monitoring data from different sources is often sparse and poorly integrated, and most of them rely on isolated stations, sometimes taken as a univocal reference for broad coastal regions. The spatial distribution of multiple variables is not necessarily enough to ecologically characterize coastal marine areas because data should conform to local attributes, i.e., human activities and the environmental disturbance they cause<sup>14,31</sup>. Yet, the integrated analysis presented in this paper, over a regional and highly detailed spatial scale, allowed us to i) identify the main ecological attributes characterizing different sub-regions; ii) relate these attributes to socio-ecological factors, including potential anthropogenic impacts from the coast; and iii) pinpoint factors that are primarily affecting the spatial-ecological distinctiveness in the study area.

Additionally, our network analysis based on the multiple correlations among the observed variables highlighted that observing the spatial behavior of some ‘primary’ variables is a necessary but not sufficient condition to assess the ecological status of a marine area comprehensively. Indeed, some secondary variables, i.e.—less correlated with other variables at the spatial scale and thus plausibly less relevant for an ecological assessment—can significantly impact specific socio-economic activities. For instance, this is the case of bacteria and meso- and protozooplankton biomasses, occupying peripheric positions in the variables’ network in Fig. 7 but affecting the food provided by the water environment to aquacultures. This condition limits the identification of a minimal yet comprehensive set of variables describing the ecological status at the regional level, supporting the need to observe and integrate multiple descriptors reciprocally and spatially to refer them to the local conditions.

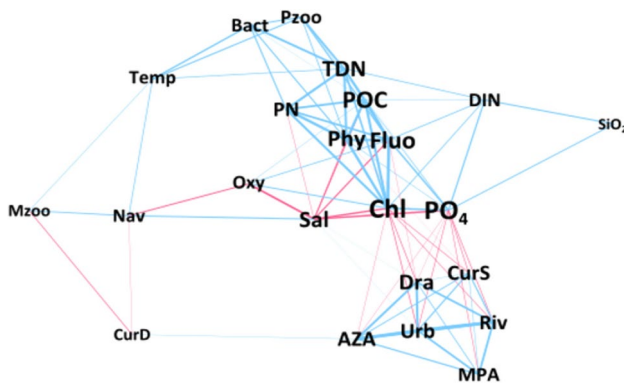


**Fig. 7.** Network visualisation of the spatial correlation among observed variables (both sampled and socio-economical) on the Campania coast. Network nodes and edges are variables and correlations among them, respectively. Node size is proportional to the node's Degree, that is, the number of correlations it establishes. Edge thickness is proportional to the correlation value. Only statistically significant correlations are presented. Red and blue lines are network edges indicating negative and positive correlations, respectively. The acronyms are as follows: AZA = Allocated zone for aquaculture; Bact = Heterotrophic bacteria; Chl = Total chlorophyll *a*; CurD = Current direction; CurS = Current speed; DIN = Dissolved inorganic nitrogen; Dra = Drain; Fluo = Fluorescence; MPA = Marine protected area; Mzoo = Mesozooplankton; Nav = Naval route; Oxy = Dissolved oxygen; Phy = Phytoplankton; PN = *Pseudo-nitzschia*; PO<sub>4</sub> = Phosphate; POC = Particulate organic carbon; Pzoo = Protozooplankton; Riv = River; Sal = Salinity; SiO<sub>2</sub> = Silicate; TDN = Total dissolved nitrogen; Temp = Temperature; Urb = Urban area.

### Spatial integration of MSFD descriptors as a priority for the coastal ecological assessment

Decision-makers need quantitative information on the worth of natural capital stocks and anthropogenic pressures—which drive, for example, the flow of ecosystem services with local specificities and dynamics—to manage and conserve coastal marine areas and their natural resources. In this context, the demand for spatial tools suitable for ecological assessments has grown over the past few decades, and GIS applications can meet these needs<sup>32</sup>.

By exploiting GIS resources in the three Campania gulfs under examination in this study, we detected that nearby marine sectors can show highly distinctive features, whereas more distant ones can be more like each other. This behavior suggests that the different variables under consideration manifest distinct and site-specific variability scales (e.g.,<sup>33</sup>). For instance, despite the relatively short distance between GoN and the farthest sampling sites, the former gulf showed a low spatial homogeneity due to the combined effect of coastal currents, forced by both geomorphology and the intrusion of Tyrrhenian waters, which transport freshwater from the Sarno River northwards. Similar sites (i.e., being at the same distance from the coastline and having similar maximum depths) showed highly distinctive environmental features. Conversely, GoS showed higher spatial homogeneity despite its geographic extension due to smoother bottom geomorphology and the higher impact of riverine input, compared to seawater transport, on the water column's ecological state.

The interaction between offshore circulation and atmospheric agents drives the water column physical dynamics in the areas investigated in this study<sup>15</sup>. Circulation mostly depends on the wind stress in autumn and winter and on the interaction with the offshore large-scale circulation and baroclinic effects, related to topographic features, during spring and summer. Both physical forces and land runoff drive fast changes in the ecological state of the water column in the Campania region, starting from the smallest living beings like plankton<sup>12,34</sup>—currently studied over the long term in the Gulf of Naples<sup>35</sup> whose ecological communities undergo fast functional shifts under such a transient physical–chemical regime<sup>36</sup>. Thus, the high spatial heterogeneity of the water column in the study area, defined by the diverse variance associated with the variables under consideration, is the tangled effect of actual seawater transport, intermittent freshwater runoff, and complex biological responses to physicochemical drivers characterizing each Campania gulf.

Many variables investigated herein (e.g., temperature, total chlorophyll *a*, planktonic organisms, microplastics) were investigated in previous studies, revealing that different tracers often show distinct spatial distribution over the same area. Our results indicate that both biomass and composition of phytoplankton point to the considerable heterogeneity of the Campania coastal waters, with the highest biomass in GoN and GoG and the lowest in GoS and coast-offshore gradients of variable shape and intensity. Against the background of a general dominance of small phytoflagellates, diatoms are a good marker of trophic conditions in the areas impacted by nutrient sources of either anthropic or riverine origin (e.g.,<sup>37</sup>). The protozooplankton compartment shows less marked differences, but an inversion of dominance from dinoflagellates to ciliates appears between GoG/GoN and GoS. Since protozoal-/mixoplankton play a key role in marine food webs<sup>38</sup>, our finding calls for a better consideration of these organisms in MSFD, such as biodiversity and food webs, which is erroneously focused on phytoplankton and mesozooplankton only.

### Holistic coastal monitoring at the spatial scale as a resource to policymakers

Our GIS approach also allowed us to identify factors, such as marine traffic lines and heterotrophic bacteria, whose interaction should be thoroughly considered in the ecological assessment of coastal marine areas, especially if aiming to select areas to establish new aquaculture plants. Marine traffic causes physical disturbance to ecosystems and can spread inorganic and organic contaminants, even far from land-based pollution sources<sup>9</sup>. The proliferation of heterotrophic bacteria is strongly associated with organic material from sewage sources and may affect seafood quality<sup>24</sup>. These negative drivers can synergistically interact in coastal marine areas hosting large naval infrastructures. A further issue emerged from the overwhelming diversity of bacterial communities floating in seawater, which may include potentially pathogenic families<sup>39</sup>. These aspects are virtually underexplored in MSFD since monitoring targets mainly heterotrophic bacteria from a quantitative point of view.

Other synergistic actions between factors can drive the ecological state of the coasts but are missed in non-holistic monitoring. For instance, due to the constant buildup of contaminants from anthropic sources, marine microscopic litter is now a worldwide sanitary problem (e.g.,<sup>40</sup>). Bacteria floating in the water column areas can exploit artificial substrates, like microplastics, to increase in number<sup>41</sup>. Microplastics are an environmental hazard as they bioaccumulate by direct or indirect ingestion/contact<sup>42</sup>. We reported that bacterial taxa attached to microplastics were like the free-living fraction, meaning they could recruit or being recruited from the surrounding environment. For instance, microplastics can be vectors of *Vibrio cholerae* (found in GoN), i.e., a dangerous human pathogen found in all microplastic samples from our survey, although with a maximum relative abundance of 0.0004%, calling for further studies. Results on polymer composition confirmed that low-density plastics, such as polypropylene, polyethylene, and polystyrene, are the most frequent at the sea surface<sup>43,44</sup>, also acting as a reservoir for seeding populations of harmful species thriving when conditions are favourable<sup>27,45</sup>. Of course, the possible presence of human/animal pathogens attached to marine microlitter can affect the decision of a site for aquaculture, as microplastics can spread from coastal areas to aquaculture sites.

Overall, the marine sectors we examined in the Campania region were different not only because they showed different physical, chemical, and biological characteristics but also because they sit at a greater or lesser distance from sources of impact or other activities: they were socio-economically distinct, e.g., in their potential in hosting aquacultures. The areas we investigated in GoN showed high levels of natural resources supporting seafood production, but they appeared more exposed to environmental and human disturbances. The areas we investigated in GoG, although less anthropized and more spatially homogeneous than those in GoN, showed peculiar trophic attributes, like a less balanced distribution of biomass across planktonic trophic levels, with potentially detrimental effects in the transfer of resources from the ecosystem to seafood production<sup>24</sup>. Finally, GoS sectors appeared less anthropized and polluted and more spatially homogeneous, even though they showed lower levels of resources. Nonetheless, these may be good aquaculture sites for filter-feeding animals. All the above-mentioned dispersed knowledge would be fundamentally missed by non-holistic monitoring, lacking both reciprocal and spatial integration of the descriptors taken into consideration.

### Conclusions and perspectives

We showed holistic monitoring in a marine coastal area, employing a dense sampling at the regional scale, and therefore capable of capturing both synergistic ecological processes and their spatial variability. This study underscores the need for an interdisciplinary approach to examine ecological functioning when assessing the ecological health of coastal areas. A coordinated and integrated approach to marine data from oceanographic surveys provides policymakers with an improved assessment of relevant legislation towards protecting citizens and the environment in marine areas<sup>46</sup>. Datasets like the one built herein and appropriate spatial analysis highlight peculiar situations not evidenced by chemical, physical, and biological analyses alone, such as the multifaceted and interacting effects of anthropogenic impact. Moreover, most long-term monitoring on marine coasts involves the sampling of a single or very few stations, failing to capture the complex spatial variability of physical, chemical, and biological variables, which is intrinsic to the marine system, due to the perpetual water movement, intermittent freshwater inputs, and the patchiness of plankton boom-bust population dynamics. Indeed, limited financial resources can direct major efforts in either time or space, either sampling one and a single point in the sea for decades or many points but rarely. This paper calls for new investigations extending the holistic approach successfully tested herein along a time series.

### Materials and methods

#### Surface dynamics

The current fields are of predominant importance for predicting the pathways of any kind of floating object, from microorganisms to particulate pollutants. To characterize the physical dynamics in the study area, we took as a reference the surface fields derived from hydrodynamic model output, along with the velocity field data provided by Copernicus Marine Environment Monitoring Service during the sampling periods.

The numerical simulations were performed using a regional ocean modeling system (Figure S3) developed for the Tyrrhenian Sea and downscaled for the Campania coastal area to obtain high-resolution simulations. It is a free-surface, terrain-following, primitive equations ocean model widely used by the scientific community for a broad range of applications<sup>47</sup> and has been recently validated for the GoN area, such as the Gulf of Naples Advanced Model using a multiannual comparison with coastal HF radar data and hydrological measurements<sup>16</sup>.

A time series of 17 years (2001–2017) of numerical simulations was used to identify the most recurrent surface circulation patterns during the sampling months (September and October). We simulated the surface current field on the Campania region domain during the September and October months from 2001 to 2017. Since the simulation for 2020 was not available due to a lack of boundary condition data, we selected 2009 as the

reference year, already used in several works on the physical and ecological context of the area at a wide range of spatial and temporal scales<sup>48–50</sup>. This analysis allowed us to have information on the main surface dynamics in the study area during the sampling periods. Data over the whole study area was used, and for each day the hourly mean data at the surface was considered for the three gulfs.

### Oceanographic surveys

Oceanographic surveys were conducted in September and October 2020 and lasted two days in each gulf. GoG, GoN, and GoS were sampled on September 9<sup>th</sup>, 10<sup>th</sup>, 17<sup>th</sup>, and 18<sup>th</sup>, and October 6<sup>th</sup> and 9<sup>th</sup> respectively. Twenty-two hydrographic stations were distributed along multiple coast-to-offshore gradients (Fig. 1; see Supplementary materials for details on sampling stations in Table S5). At each station, samples for physical, chemical, and biological characterisation and microplastics were collected (Table S1).

### Physical and chemical variables

At each hydrographic station, conductivity, temperature, and depth data were obtained with a SeaBird 911 Plus multi-parametric probe with temperature and conductivity sensors and further auxiliary sensors for dissolved oxygen, salinity, fluorescence, turbidity, and PAR (Photosynthetically Active Radiation). Calibration parameters were applied after checking the agreement with salinity bottle samples. For each station, the physical variables were gathered in a near-continuous mode during the entire cast, providing 24 Hz sampling with an SBE 9plus conductivity, temperature, and depth unit and SBE 11plus V2 deck unit.

Sea water Samples were collected using Niskin bottles for the determination of dissolved inorganic nutrients (nitrite =  $\text{NO}_2^-$ ; nitrate =  $\text{NO}_3^-$ ; ammonia =  $\text{NH}_3$ ) concentrations ( $\text{mmol m}^{-3}$ ) and immediately stored in 20 mL HDPE vials at  $-20^\circ\text{C}$ . The analyses were carried out with a continuous flow autoanalyzer (Flow-Sys Systea), based on an updated version of the protocol developed by Hansen and Grasshoff<sup>51</sup>. The concentration of dissolved inorganic nitrogen was calculated as  $\text{NO}_3^- + \text{NO}_2^- + \text{NH}_4^+$ . Samples for the determination of total dissolved nitrogen and phosphorus were pre-filtered with acetate cellulose membranes (Whatman) and collected in 100 mL HDPE containers, stored at  $-20^\circ\text{C}$ . Total dissolved nitrogen and phosphorus concentrations were measured with the persulfate oxidation method (digestion at  $120^\circ\text{C}$  for 30 min) followed by the determination of nitrate and phosphate, using the improvements proposed by Valderrama<sup>52</sup> to the original methods by Koroleff<sup>53,54</sup>.

To determine particulate organic carbon and particulate nitrogen concentrations ( $\text{mg m}^{-3}$ ), variable volumes (0.7–2 L) of seawater were filtered on Whatman GF/F pre-combusted ( $450^\circ\text{C}$ , 5 h) glass fiber filters immediately stored at  $-20^\circ\text{C}$  after collection. To remove the inorganic carbonate fraction, filters were exposed overnight to HCl vapors and then analysed with a Thermo Electron CHN elemental analyzer (FlashEA 1112 Series)<sup>55</sup>.

### Plankton sampling and counting

The main biological variables determined at all sampling sites consisted of the abundance of prokaryotic and eukaryotic plankton in the water column, these organisms being divided between protists (unicellular, both photosynthetic and heterotrophic) and metazoans. Herein, we refer to photosynthetic and heterotrophic protists as phytoplankton and protozooplankton, respectively, and to metazoans as mesozooplankton (the 200–20,000  $\mu\text{m}$  size fraction). At selected stations, we also analysed seed banks on the bottom sediments and the microbiota associated with microplastics. This information allowed us to assess the potential productivity levels of the water column sustaining aquaculture and fisheries in different sectors of the Campania coast, as well as the potential biotic threats to these activities.

As for planktonic prokaryotes, duplicate seawater samples for flow cytometry (1 mL each) were placed in 2.0 mL cryovials, fixed with a mix of glutaraldehyde and paraformaldehyde (0.05% and 1% final concentrations, respectively) for 10 min in the dark, frozen in liquid nitrogen, and stored at  $-80^\circ\text{C}$  until analysis<sup>56</sup>. Total abundances were determined using a BD FACSVerso flow cytometer (BD Biosciences, Franklin Lake, USA) equipped with a 488 nm laser excitation and the standard filter setup. Analysis of heterotrophic prokaryotes was performed after thawing and staining the samples with SYBRGreen I (Molecular Probes, Inc., USA) as described in Balestra et al.<sup>57</sup>. Heterotrophic prokaryotes were discriminated from other particles or backgrounds based on side scatter and by their green fluorescence from SYBRGreen I, which was also used to discriminate HNA (High Nucleic Acid content) from LNA (Low Nucleic Acid content) prokaryotic cells<sup>58</sup>. Data acquisition and file analysis were performed using the software FACSuite (BD Biosciences, Franklin Lake, USA) and FCS Express 6 Flow v 6.06.0025 (DeNovo Software, Glendale, USA), respectively.

For the analysis of the total chlorophyll *a* (a proxy of phytoplankton biomass) and its pico-, nano-, and micro-size fractions (< 2, 2–20, and > 20  $\mu\text{m}$ ; respectively), 500 mL of seawater were filtered on board through Whatman GF/F and Nucleopore membrane filters (25 mm diameter) and rapidly frozen at  $-80^\circ\text{C}$ . Sample fractionation was performed following a protocol of serial filtration as reported by Mangoni et al.<sup>59</sup>. Frozen filters were processed for the determination of the total chlorophyll *a* and phaeopigments content using a solution of 90% acetone according to Holm-Hansen et al.<sup>60</sup>, with a spectrofluorometer (Shimadzu, Mod.RF-6000; Shimadzu Corporation-Japan) checked daily with a chlorophyll standard solution (Sigma-Aldrich). The percentage contribution of each size class (see above) was calculated.

Water samples for quantitative analyses of phyto- and protozooplankton were collected from Niskin bottles at 0 m and 10 m depths. Additional samples for detection of rare species were collected with a 20  $\mu\text{m}$  mesh-size net towed horizontally in surface waters for about 5 min. Seawater from the Niskin bottles and the net haul were gently poured into 250- and 100-mL dark glass bottles, respectively, previously filled with Lugol's iodine solution (1% final concentration). As for phytoplankton, 5–100 mL (depending on cell concentration) were settled in Utermöhl chambers. For protozooplankton, samples were settled in a graduated cylinder for 48 h and concentrated to 100 mL by gently collecting the supernatant. The concentrated samples were allowed to settle in sedimentation chambers for 48 h. Specimens' identification and counts were performed according

to the Utermöhl method<sup>61</sup> with an inverted light microscope Zeiss Axiovert 200 (Carl Zeiss, Germany) at 40x (phytoplankton) and 20x (protozooplankton) magnifications. Among dinoflagellates, small-sized (< 15 µm) dinoflagellates were considered in phytoplankton analysis, and large-sized (> 15 µm) dinoflagellates were counted in protozooplankton analysis. Taxonomic identification was performed at the species level whenever possible according to the most relevant and updated taxonomic literature. Carbon content for the two categories was estimated from mean cell bio-volumes using the formulas proposed by Menden-Deuer<sup>62</sup>.

Mesozooplankton samples were collected at all stations with vertically integrated tows from 5 m above the sea bottom to the surface with a double WP2 net (0.25 m<sup>2</sup> mouth area, 200 µm mesh size) equipped with a flowmeter. The samples were transferred from the cod-end to two 500 mL plastic jars, then each one was gently filtered through 100 µm mesh size and fixed in ethanol 96% and in formaldehyde (4%). Each sample in ethanol was concentrated and then resuspended in a bowl with distilled water to a final volume of 200 mL; two aliquots of 5 mL each were analysed using a stereomicroscope (Leica MZ 12.5) in a 10 mL Bogorov counting chamber. Taxonomic identification was performed at the species level whenever possible according to the most relevant and updated taxonomic literature (e.g.,<sup>63</sup>). Mesozooplankton biomass was estimated by considering the individual carbon content (µg C ind.<sup>-1</sup>) for each identified taxon, based on our unpublished measurements or taken from the literature. Total mesozooplankton biomass (mg C m<sup>-3</sup>) was calculated by multiplying, for each taxon, individual carbon content by taxon abundance, then summing the biomass of all taxa.

### Sediment sampling, DNA extraction, and sequencing

Sediments were collected with a gravity corer equipped with three collectors, each 4 cm in diameter, at the mouth of the Volturno River in the GoG (FE\_8 at 47 m depth) on 10 th September 2020 and at the mouth of the Sarno River in the GoN (FE\_16 at 50 m depth) on 18 th September 2020. The surface sediments (0–1 cm) of each collector were pooled together, gently mixed, and placed in a 50 mL Falcon tube, which was stored in the dark at 4 °C for 7 weeks to ensure that only the resting stages of planktonic organisms survived.

One subsample of 5 g of surface sediment was used to extract DNA with the PowerMax™ soil DNA isolation kits (MoBio, Laboratories, U.S.). DNA yield and purity were evaluated by Qubit 2.0 fluorometer Invitrogen (Thermo Scientific, U.S.). The V4 region of the eukaryotic SSU rDNA gene was amplified as illustrated in Piredda<sup>64</sup> and sequenced with Illumina MiSeq sequencing at LGC Genomics GmbH (Berlin, Germany). Amplicon Sequence Variants were generated as follows: quality metrics of demultiplexed reads were first assessed using FastQC. Reads were trimmed with cutadapt<sup>65</sup> as follows: in the first round, 5' primers were trimmed, discarding reads if the primer was not found; in the second round 3' primers were trimmed, but keeping the reads without primers. In both rounds, adapter mismatch was set at 0.25, and terminal Ns were removed if present. The two-stage procedure avoids discarding read pairs from amplicons sized between 250 and 490 bp, long enough for the reads to overlap but where 3' primers are truncated or absent.

Contig assembly, denoising, dereplication, and chimera screening were performed with the DADA2 R package<sup>66</sup>, using the default parameters described in the MiSeq tutorial, except for allowing up to 6 mismatches in read merging (function mergePairs, parameter: maxMismatch = 6). Resulting amplicon sequence variants were then classified with BLAST using an identity cutoff of 97% against the PR2 v4.12 reference database<sup>67</sup> integrated with private sequences. All nucleotide sequences will be available in the European Nucleotide Archive upon publication.

### Microplastics and the microbial plastisphere

Seawater samples (in triplicates) and microplastic samples were taken at stations FE13 (GoN), FE1-FE2-FE8 (GoG), and FE18-FE24 (GoS). Microplastic samples were collected according to MSFD guidelines<sup>68</sup> modified according to Fossi et al.<sup>69</sup> with a Hyponeuston Manta Trawl (mouth opening: 16 × 60 cm; 330 µm mesh size; Oceomic Inc., Spain), equipped with a flow-meter (Model 23.090, KC Denmark A/S, Denmark), and towed for 30 min at an average speed of 2 knots or less. Once removed, the cod-end content was sieved through 5000 and 300 µm in sequence. The largest microplastics within 300 and 5000 µm were removed with sterile forceps, rinsed with 0.22 µm filter-sterilised seawater, and cut into two parts, one of which was used for DNA extraction and the other for chemical composition by Fourier-Transform Infrared Spectroscopy (FT-IR). The remaining microplastics on the smaller sieve (300–5000 µm), together with all organic and inorganic material, including zooplankton and other organisms, were then poured into a glass jar, fixed with 70% ethanol, and stored at 4 °C for counting.

Once in the lab, samples were poured into a Petri dish, and microplastics were counted and classified using a stereomicroscope (Leica CLS 150 XE, 20–80 × magnification). Microplastic abundance data, for each sampling site, were normalised to the total volume of filtered water and expressed as items m<sup>-3</sup>. About 1 L of seawater from each sampling station was filtered through mixed cellulose ester filters (GSWP04700, Millipore, USA) in triplicate. DNA was extracted from either plastic pieces or filters (to compare with the microplastic-attached microbes) using the Puregene Tissue DNA extraction kit (Qiagen, Valencia, CA) with a modified bead-beating procedure<sup>45</sup>. The extracted DNA was sequenced with Illumina MiSeq sequencing for the V4 and V5 hypervariable regions of the 16SrRNA gene<sup>70</sup> and for the V4 hypervariable region of the 18S RNA gene of eukaryotes<sup>71</sup>. The results were preprocessed using the GAIA software from Sequentia Biotech<sup>72</sup>. All nucleotide sequences will be made available through a reasoned request to the corresponding authors.

### GIS analysis

All data collected during oceanographic surveys were imported into ArcGIS v. 10.8 (<https://www.esri.com/e-n-us/home>) to create raster maps for physical, chemical, and biological variables. From raw data, we obtained shapefiles of sampling sites that were projected in the WGS 84 coordinate system with the ArcGIS tool “Projections and Transformations”. The coordinate system of each variable dataset was used throughout ArcGIS

to display, measure, and transform geographic data. For each variable, a raster map was produced throughout the interpolation analysis of data in sampling sites, integrating values at depths of 0 and 10 m by the tool “Spline with Barriers”. This method interpolates a raster surface using barriers from points using a minimum curvature spline technique. The barriers were entered either as polygon or polyline features. All raster maps had a grid resolution of 1.36 km × 1.36 km. The pixel resolution of maps was chosen considering the distance between sampled points by using the mean shortest distance method following Hengl<sup>73</sup>.

For the GIS analysis, a raster map of the variable distance of the following layers was generated:

- Urban area (source: <https://land.copernicus.eu/pan-european/corine-land-cover/clc2018>);
- Marine Protected Areas (source: <https://www.iucn.org/theme/protected-areas/our-work/world-database-protected-areas>);
- Allocated Zone for aquaculture (source: <https://geoportal.bioinfo.szn.it/>), Sea route (source: <https://geoport.al.bioinfo.szn.it/>);
- Rivers (source: [http://ihp-wins.unesco.org/layers/geonode:world\\_rivers](http://ihp-wins.unesco.org/layers/geonode:world_rivers)) and drains (source: <https://www.arpacampania.it/database-georeferenziato-scarichi-costieri>).

This distance was obtained by using the tools “Near”, which calculates the distance and additional proximity information between the input features and the closest feature in another layer or feature class. The distance was calculated in km with the geodesic method to consider the curvature of the spheroid and appropriately deals with data near the dateline and poles. The tool “Band Collection Statistics” was used to calculate the statistics for a set of raster bands and analyze the correlation between all the raster maps. Then, we imported the correlation table in Excel to obtain a p-value matrix for each r value.

### Statistical analysis

The correlation analysis matrix for the chemical, physical, and biological variables was carried out in XLstat. Correlation matrices were visualised as networks with the open-source software Gephi<sup>74</sup> using the Yifan Hu algorithm, which provides good performance and readability for small networks<sup>75</sup>. To provide a synthetic view of the multiple interrelations among the variables observed, we correlated all variables at the regional scale and derived a network including only statistically significant correlations (Pearson’s coefficient of correlation), both positive and negative ones. Two network metrics were calculated to rank the nodes based on their network relevance<sup>76</sup>: i) degree index, i.e., the total number of connections (here correlations) established with other nodes and describing the centrality of a node in terms of its positional importance based on its direct interactions; and ii) betweenness centrality, i.e., the average number of times a node acts as a bridge along the shortest path between two nodes (Table S6).

Patterns of divergence among the three gulfs were explored using 24 variables and data extrapolated from the GIS maps, applying PCA to data scaled to have unit variance in the R package factoextra v. 1.0.7 (<https://github.com/kassambara/factoextra>) and stats v. 4.0.3<sup>77</sup>). We performed PCA considering all the variables, only physical variables, only chemical variables, and only biological variables in R (a language and environment for statistical computing—R Foundation for Statistical Computing, Vienna, Austria. URL <https://www.R-project.org/>). The significance of differences observed among the three gulfs based on the 24 studied variables was verified through Welch ANOVA and the Games-Howell post-hoc test as data deviated from normality and homoscedasticity according to the Shapiro and Levene test in the R package matrixTest v. 0.1.9.1 (<https://github.com/karoliskonc/matrixTests>).

### Data availability

The datasets used and/or analysed during the current study are available from the corresponding author upon reasonable request.

Received: 9 April 2024; Accepted: 25 April 2025

Published online: 09 May 2025

### References

1. Livingston, R. J. *Trophic organization in coastal systems*. CRC Press (2002).
2. He, Q. & Silliman, B. R. Climate change, human impacts, and coastal ecosystems in the anthropocene. *Curr. Biol.* **29**, R1021–R1035 (2019).
3. Selig, E. R. et al. Mapping global human dependence on marine ecosystems. *Conserv. Lett.* **12**, e12617 (2019).
4. Halpern, B. S. et al. A global map of human impact on marine ecosystems. *Science* **319**, 948–952 (2008).
5. D’Alelio, D., Russo, L., Hay Mele, B. & Pomati, F. Intersecting ecosystem services across the aquatic continuum: From global change impacts to local, and biologically driven, synergies and trade-offs. *Front. Ecol. Evol.* **9**, 628658 (2021).
6. Boyes, S. J., Elliott, M., Murillas-Maza, A., Papadopoulou, N. & UyarraIs, M. C. Is existing legislation fit-for-purpose to achieve good environmental status in European seas? *Mar. Pollut. Bull.* **111**, 18–32 (2016).
7. Appolloni, L., Sandulli, R., Vetrano, G. & Russo, G. F. A new approach to assess marine opportunity costs and monetary values-in-use for spatial planning and conservation; the case study of Gulf of Naples, Mediterranean Sea. *Italy: Ocean Coast. Manag.* **152**, 135–144 (2018).
8. Mattei, G., Rizzo, A., Anfuso, G., Aucelli, P. P. C. & Gracia, F. J. A tool for evaluating the archaeological heritage vulnerability to coastal processes: The case study of Naples Gulf (southern Italy). *Ocean Coast. Manag* **179**, 104876 (2019).
9. Tornero, V., Ribera, M. & d’Alcalà, Contamination by hazardous substances in the Gulf of Naples and nearby coastal areas: A review of sources, environmental levels and potential impacts in the MSFD perspective. *Sci. Total Environ.* **1**, 466–467 (2014).
10. Cianelli, D. et al. Dynamics of a very special Mediterranean coastal area: the Gulf of Naples. In *Mediterranean ecosystems* (ed. Williams, G. S.) 129–150 (Nova Science Publishers, Inc., 2012).
11. Gifuni, L., de Ruggiero, P., Cianelli, D., Pierini, S. & Zambianchi, E. Numerical investigation of the three-dimensional paths of plastic polymers in the Gulf of Naples. *Mar. Pollut. Bull.* **193**, 115259 (2023).

12. Cianelli, D. et al. Disentangling physical and biological drivers of phytoplankton dynamics in a coastal system. *Sci. Rep.* **7**, 15868 (2017).
13. D'Alelio, D., Hay, B., Libralato, M. S., Ribera d'Alcalà, M. & Ferenc, J. Rewiring and indirect effects underpin modularity reshuffling in a marine food web under environmental shifts. *Ecol. Evol.* **9**, 11631–11646 (2019).
14. Hay Mele, B., Russo, L. & D'Alelio, D. Combining marine ecology and economy to roadmap the integrated coastal management: a systematic literature review. *Sustainability* **11**, 4393 (2019).
15. Iacono, R., Napolitano, E., Palma, M. & Sannino, G. The tyrrhenian sea circulation: A review of recent work. *Sustainability* **13**, 6371 (2021).
16. Kokoszka, F. et al. Gulf of Naples Advanced Model (GNAM): A multiannual comparison with coastal HF radar data and hydrological measurements in a coastal Tyrrhenian Basin. *J. Mar. Sci. Eng.* **10**, 1044 (2022).
17. Garmendia, M., Borja, Á., Franco, J. & Revilla, M. Phytoplankton composition indicators for the assessment of eutrophication in marine waters: Present state and challenges within the European directives. *Mar. Pollut. Bull.* **66**, 7–16 (2012).
18. Ibáñez, C. et al. Ecosystem-level effects of re-oligotrophication and N: P imbalances in rivers and estuaries on a global scale. *Glob. Chang. Biol.* **29**, 1248–1266 (2023).
19. Beaugrand, G. Monitoring pelagic ecosystems using plankton indicators. *ICES J. Mar. Sci.* **62**, 333–338 (2005).
20. Brown, A. R. et al. Assessing risks and mitigating impacts of harmful algal blooms on mariculture and marine fisheries. *Rev. Aquac.* **12**, 1663–1684 (2020).
21. Flynn, K. J. et al. Mixotrophic protists and a new paradigm for marine ecology: where does plankton research go now?. *J. Plankton Res.* **41**, 375–391 (2019).
22. Wang, Z. et al. Metabarcoding of harmful algal bloom species in sediments from four coastal areas of the southeast China. *Front. Microbiol.* **13**, 99986 (2022).
23. Rombouts, I. et al. Food web indicators under the marine strategy framework directive: From complexity to simplicity?. *Ecol. Indic.* **29**(246), 254 (2013).
24. Kang, H. C. et al. Food web structure for high carbon retention in marine plankton communities. *Sci. Adv.* **9**, eadk0842 (2023).
25. Alberghini, L., Truant, A., Santonicola, S., Colavita, G. & Giaccone, V. Microplastics in fish and fishery products and risks for human health: A review. *Int. J. Environ. Res. Public Health* **20**(1), 789 (2022).
26. Curren, E., Leaw, C. P., Lim, P. T. & Leong, S. C. Y. Evidence of marine microplastics in commercially harvested seafood. *Front. Bioeng. Biotechnol.* **4**, 562760 (2020).
27. Amaral-Zettler, L. A. et al. Diversity and predicted inter-and intra-domain interactions in the mediterranean plastisphere. *Environ. Pollut.* **286**, 117439 (2021).
28. Bartlett, D. & Sudarshana, R. Cultural intermixing, the diffusion of GIS and its application to coastal management in developing countries. *GIS Coast. Zone Manag.* <https://doi.org/10.1201/9781420023428.ch12> (2004).
29. Bosso, L. et al. Geoports in marine spatial planning: state of the art and future perspectives. *Ocean Coast. Manag.* **266**, 107688 (2025).
30. Noble, M. M., Harasti, D., Pittock, J. & Doran, B. Linking the social to the ecological using GIS methods in marine spatial planning and management to support resilience: a review. *Mar. Policy* **108**, 103657 (2019).
31. Mele, B. H. et al. Ecological assessment of anthropogenic impact in marine ecosystems: the case of Bagnoli Bay. *Mar. Environ. Res.* **158**, 104953 (2020).
32. Patera, A., Pataki, Z. & Kitsiou, D. Development of a webGIS application to assess conflicting activities in the framework of marine spatial planning. *J. Mar. Sci. Eng.* **10**, 389 (2022).
33. Moses, W. J., Ackleson, S. G., Hair, J. W., Hostetler, C. A. & Miller, W. D. Spatial scales of optical variability in the coastal ocean: Implications for remote sensing and in situ sampling. *J. Geophys. Res.: Oceans* **121**, 4194–4208 (2016).
34. Ciannelli, L. et al. Ichthyoplankton assemblages and physical characteristics of two submarine canyons in the south-central Tyrrhenian Sea. *Fish. Oceanogr.* **31**, 480–496 (2022).
35. Zingone, A., D'Alelio, D., Mazzocchi, M. G., Montresor, M. & Sarno, D. Time series and beyond: multifaceted plankton research at a marine Mediterranean LTER site. *Nat. Conserv.* **34**, 273–310 (2019).
36. D'Alelio, D. et al. Ecological-network models link diversity, structure and function in the plankton food-web. *Sci. Rep.* **6**, 21806 (2016).
37. Lu, X., Zhang, Y., Liu, Y. & Fan, Y. Differences in planktonic and benthic diatoms reflect water quality during a rainstorm event in the Songhua River Basin of northeast China. *Ecol. Indic.* **144**, 109547 (2022).
38. Mansour, J. S. & Anestis, K. Eco-evolutionary perspectives on mixoplankton. *Front. Mar. Sci.* **8**, 666160 (2021).
39. Basili, M., Campanelli, A., Frapiccini, E., Luna, G. M. & Quero, G. M. Occurrence and distribution of microbial pollutants in coastal areas of the Adriatic Sea influenced by river discharge. *Environ. Pollut.* **285**, 117672 (2021).
40. Chatziparaskeva, G., Papamichael, I. & Zorbas, A. A. Microplastics in the coastal environment of mediterranean and the impact on sustainability level. *Sustain. Chem. Pharm.* **29**, 100768 (2022).
41. Parsaeimehr, A., Miller, C. M. & Ozbay, G. Microplastics and their interactions with microbiota. *Heliyon* **9**, e15104 (2023).
42. Squillante, J. et al. Occurrence of phthalate esters and preliminary data on microplastics in fish from the Tyrrhenian sea (Italy) and impact on human health. *Environ. Pollut.* **316**, 120664 (2023).
43. Andrade, A. L. Microplastics in the marine environment. *Mar. Pollut. Bull.* **62**, 1596–1605 (2011).
44. Suaria, G. et al. The mediterranean plastic soup: Synthetic polymers in Mediterranean surface waters. *Sci. Rep.* **6**, 37551 (2016).
45. Zettler, E. R., Mincer, T. J. & Amaral-Zettler, L. A. Life in the “plastisphere”: microbial communities on plastic marine debris. *Environ. Sci. Technol.* **47**, 7137–7146 (2013).
46. Drakopoulos, L., Havice, E. & Campbell, L. Architecture, agency and ocean data science initiatives: Data-driven transformation of oceans governance. *Earth Syst. Govern.* **12**, 100140 (2022).
47. Haidvogel, D. B. et al. Ocean forecasting in terrain-following coordinates: Formulation and skill assessment of the regional ocean modeling system. *J. Comput. Phys.* **227**, 3595–3624 (2008).
48. Uttieri, M. et al. Multiplatform observation of the surface circulation in the Gulf of Naples (Southern Tyrrhenian Sea). *Ocean Dyn.* **61**, 779–796 (2011).
49. Saviano, S. et al. Sea storm analysis: Evaluation of multiannual wave parameters retrieved from HF radar and wave model. *Remote Sens.* **14**, 1696 (2022).
50. Saviano, S. et al. Wind direction data from a coastal HF radar system in the Gulf of Naples (Central Mediterranean Sea). *Remote Sens.* **13**, 1333 (2021).
51. Hansen, H.P. & Grasshoff K. Automated chemical analysis. *Meth. Seaw. Anal.* 347–395 (1983).
52. Valderrama, J. C. The simultaneous analysis of total nitrogen and total phosphorus in natural sea-waters. *Mar. Chem.* **10**, 109–122 (1981).
53. Koroleff, F. Total and organic nitrogen. In *Methods of Seawater Analysis* (ed. Grasshoff, K.) 167–173 (Verlag Chemie, 1976).
54. Koroleff, F. Determination of total phosphorus. In *Methods of Seawater Analysis* (ed. Grasshoff, K.) 123–125 (Verlag Chemie, 1976).
55. Hedges, J. I. & Stern, J. H. Carbon and nitrogen determinations of carbonate-containing solids. *Limnol. Oceanogr.* **29**, 657–663 (1984).
56. Marie, D., Partensky, F., Vaulot, D. & Brussard, C. Enumeration of phytoplankton, bacteria, and viruses in marine samples. *Curr. Protoc. Cytom.* **10**, 11–11 (1999).

57. Balestra, C., Alonso-Sáez, L., Gasol, J. M. & Casotti, R. Group-specific effects on coastal bacterioplankton of polyunsaturated aldehydes produced by diatoms. *Aquat. Microb. Ecol.* **63**, 123–131 (2011).
58. Gasol, J. M. & Del Giorgio, P. A. Using flow cytometry for counting natural planktonic bacteria and understanding the structure of planktonic bacterial communities. *Sci. Mar.* **64**, 197–224 (2000).
59. Mangoni, O. et al. Phytoplankton blooms during austral summer in the Ross Sea, Antarctica: Driving factors and trophic implications. *PLoS ONE* **12**, e0176033 (2017).
60. Holm-Hansen, O., Lorenzen, C. J., Holmes, R. W. & Strickland, J. D. Fluorometric determination of chlorophyll. *ICES J. Mar. Sci.* **30**, 3–15 (1965).
61. Edler, L. & Elbrächter, M. The Utermöhl method for quantitative phytoplankton analysis. In Karlson, B., Cusack, C.K. & Bresnan, E. *Microscopic and molecular methods for quantitative phytoplankton analysis*. UNESCO Paris 13–20 (2010)
62. Menden-Deuer, S. & Lessard, E. J. Carbon to volume relationships for dinoflagellates, diatoms, and other protist plankton. *Limnol. Oceanogr.* **45**, 569–579 (2000).
63. Castellani, C. & Edwards, M (A practical guide to ecology, methodology, and taxonomy. Oxford University Press, 2017).
64. Piredda, R. et al. Diversity and temporal patterns of planktonic protist assemblages at a Mediterranean Long Term Ecological Research site. *FEMS Microbiol. Ecol.* **93**, fiw200 (2017).
65. Martin, M. Cutadapt removes adapter sequences from high-throughput sequencing reads. *EMBnet. J.* **17**, 10–12 (2011).
66. Callahan, B. J. et al. DADA2: high-resolution sample inference from Illumina amplicon data. *Nat. Meth.* **13**, 581 (2016).
67. Guillou, L. et al. The Protist Ribosomal Reference database (PR2): A catalog of unicellular eukaryote Small Sub-Unit rRNA sequences with curated taxonomy. *Nucleic Acids Res.* **41**, D597–D604 (2012).
68. Galgani, F., Giorgetti, A., Vinci, M., Le Moigne, M., Moncoiffe, G., Brosich, A., Molina, E., Lipizer, M., Holdsworth, N., Schlitzer, R., Hanke, G., Schaap, D. Proposal for gathering and managing data sets on marine micro-litter on a European scale 34 (2019)
69. Fossi, M.C. et al. Toolkit for monitoring marine litter and its impacts on biodiversity in Mediterranean MPAs. Interreg Med Plastic Busters MPAs project (D.3.3.2) (2019).
70. Parada, A. E., Needham, D. M. & Fuhrman, J. A. Every base matters: Assessing small subunit rRNA primers for marine microbiomes with mock communities, time series and global field samples. *Environ. Microbiol.* **18**, 1403–1414. <https://doi.org/10.1111/1462-2920.13023> (2016).
71. Hugoni, M., Luis, P., Guyonnet, J. & Haichar, F. E. Z. Plant host habitat and root exudates shape fungal diversity. *Mycorrhiza* **28**, 451–463 (2018).
72. Apine, E. et al. Comparative analysis of the intestinal bacterial communities in mud crab *Scylla serrata* in South India. *MicrobiologyOpen* **10**, e1179 (2021).
73. Hengl, T. Finding the right pixel size. *Comput. Geosc.* **32**, 1283–1298 (2006).
74. Bastian, M., Heymann, S. & Jacomy, M. Gephi: An open source software for exploring and manipulating networks. BT - International AAAI Conf. on weblogs and social. *Int. AAAI Conf. Weblogs Soc. Media* **3** 361–362. (2009).
75. Jacomy, M., Venturini, T., Heymann, S. & Bastian, M. ForceAtlas2, a continuous graph layout algorithm for handy network visualization designed for the Gephi software. *PLoS ONE* **9**, 1–12 (2014).
76. Wasserman, S. & Faust, K. *Social network analysis: Methods and applications* (Cambridge University Press, 1994).
77. R v. 4.0.3 (R Core Team (2020). R: A language and environment for statistical computing. R Foundation for Statistical Computing, Vienna, Austria. URL <https://www.R-project.org/>) was used in all these analyses.

## Author contributions

L.B., S.S., D.C., D.D.—Conceptualization; Methodology; Validation; Formal Analysis; Investigation; Resources; Data Curation; Writing – Original Draft Preparation; Writing – Review & Editing; Supervision. M. A., D.B., F.B., V.B., A.B., Y.C., R.C., M.L.C., F.C., F.D.D., G.D.G., V.D., M.F., D.I., F.K., F.L., P.L., O.M., F.M., M.G.M., M.M., M.M., M.P., C.P., I.P., F.R., L.R., T.R., M.S., D.S., A.C.T., J.V., M.V.G.Z., A.Z.—Methodology; Formal Analysis; Investigation; Writing – Original Draft Preparation; Writing – Review & Editing.

## Funding

The present study was supported by: 1) the projects ISSPA—PO FEAMP Campania 2014–2020 (DRD n. 35 of 15 th March 2018) and EuroSea project (N° 862626); and 2) the National Recovery and Resilience Plan (NRRP), Mission 4 Component 2 Investment 1.4—Call for tender No. 3138 of 16 December 2021, rectified by Decree n.3175 of 18 December 2021 of Italian Ministry of University and Research funded by the European Union – NextGenerationEU; Project code CN\_00000033, Concession Decree No. 1034 of 17 June 2022 adopted by the Italian Ministry of University and Research, CUP, H43 C22000530001, Project title “National Biodiversity Future Center—NBFC”.

## Declarations

### Competing interests

The authors declare no competing interests.

### Additional information

**Supplementary Information** The online version contains supplementary material available at <https://doi.org/10.1038/s41598-025-00206-z>.

**Correspondence** and requests for materials should be addressed to D.C. or D.D.

**Reprints and permissions information** is available at [www.nature.com/reprints](http://www.nature.com/reprints).

**Publisher's note** Springer Nature remains neutral with regard to jurisdictional claims in published maps and institutional affiliations.

**Open Access** This article is licensed under a Creative Commons Attribution-NonCommercial-NoDerivatives 4.0 International License, which permits any non-commercial use, sharing, distribution and reproduction in any medium or format, as long as you give appropriate credit to the original author(s) and the source, provide a link to the Creative Commons licence, and indicate if you modified the licensed material. You do not have permission under this licence to share adapted material derived from this article or parts of it. The images or other third party material in this article are included in the article's Creative Commons licence, unless indicated otherwise in a credit line to the material. If material is not included in the article's Creative Commons licence and your intended use is not permitted by statutory regulation or exceeds the permitted use, you will need to obtain permission directly from the copyright holder. To view a copy of this licence, visit <http://creativecommons.org/licenses/by-nc-nd/4.0/>.

© The Author(s) 2025